Effect of Electron Collisions on Ion-Acoustic Waves and Heat Flow

Introduction

The damping rate of ion-acoustic waves in plasma plays an important role in establishing the threshold for the onset of stimulated Brillouin scattering, ion-temperature-gradient instability, current-driven ion-acoustic instability, and other drift-wave microinstabilities. The effect of electron-ion (*e-i*) collisions on the ion-acoustic damping rate has been recently investigated by analytically solving the electron Fokker-Planck (FP) equation for a Lorentz plasma (i.e., neglecting *e-e* collisions) with cold ions and arbitrary $k\lambda_{ei}$ (where k is the wave number and λ_{ei} is the *e-i* mean free path).[1] It was shown that, as *e-i* collisions are introduced, the damping rate γ rises monotonically above the collisionless Landau limit γ_Λ, reaches a peak at $k\lambda_{ei} \sim \left(Zm_e/m_i\right)^{1/2}$ (where Z is the charge number and m is the mass), and then decreases to zero as $k\lambda_{ei} \rightarrow 0$ with the damping rate γ_{fluid} predicted by fluid theory.

The main purpose of this article is to assess the contributions from both *e-e* and *e-i* collisions on the damping of the ion-acoustic waves. Results are based on numerical simulations using a code (*SPRING*) that solves the linearized electron FP and cold-ion fluid equations. We are able to explore a wide range of values of $k\lambda_{ei}$ and Z by expanding the electron-distribution function in an arbitrary number of Legendre modes, and by using the *exact* form of the Rosenbluth[2] potentials (neglecting terms of the order of m_e/m_i). In the high-Z limit, where *e-e* collisions can be ignored, the analytic Lorentz-plasma results of Epperlein *et al.*[1] are recovered. For low-Z plasmas, *e-e* collisions become significant and promote a reduction in the damping near $k\lambda_{ei} = 1$, though γ still remains larger than γ_L and γ_{fluid}. The approximation of isotropic Rosenbluth potentials is also investigated and found to yield sufficiently accurate values of γ (error <10%). A further useful approximation that involves adjusting the *e-i* collision frequency to simulate the strength of *e-e* collisions is shown to be similarly accurate. Although finite ion-temperature effects have been neglected in the current analysis, their contribution to γ has been investigated by Randall[3] and more recently by Tracy *et al.*,[4] who calculated the ion-acoustic eigenfrequency ω for arbitrary $k\lambda_{ii}$ (where λ_{ii} is the *i-i* mean free path) and isothermal electrons.

It is also of interest to calculate the effective (or generalized) thermal conductivity κ based on the perturbed distribution function and compare it to the classical Spitzer-Härm (SH)[5] conductivity κ_{SH}. Not only does this give insight into electron kinetic effects, but it can also provide a way of incorporating kinetic effects into fluid equations. This idea has been successfully used in the context of electron heat transport in laser-produced plasmas[6] and more recently in the context of drift-wave microinstabilities in tokamak plasmas.[7,8] In particular, generalized thermal conductivities have been calculated by Hammett and Perkins[7] (κ_{HP}) for collisionless plasmas, and by Chang and Callen[8] for arbitrary $k\lambda_{ei}$, ω, and Z.

The results for κ calculated here are shown to reproduce the analytic results of Epperlein *et al.*[1] obtained in the Lorentz plasma approximation. In the collisional limit ($k\lambda_{ei} << 1$) κ approaches κ_{SH}, and in the collisionless limit ($k\lambda_{ei} >> 1$) it approaches κ_{HP}. We find, however, significant discrepancies with the results of Chang and Callen. They underestimate κ by factors ranging from 2.4 (at $Z = 1$) to 7.1 (as $Z \rightarrow \infty$) in the collisional limit.

The introduction of a spatially modulated inverse-bremsstrahlung heating source has also been recently shown to significantly reduce the effectiveness of heat conduction when $k\lambda_{ei} >> 1$.[9] A simple analytic formula for $\kappa_{\text{IB}}/\kappa_{\text{SH}}$ as a function of $k\lambda_{ei}$ has been proposed, based on simulations with an approximate form of the FP equation. Here we are able to assess the accuracy of the κ_{IB} formula and show that the reduction in conductivity (relative κ_{SH}) for $k\lambda_{ei} >> 1$ is indeed larger than for the undriven case, with freely propagating sound waves.

In the following sections, we describe the electron FP and cold-ion fluid equations and the numerical scheme (*SPRING* code) adopted for their solution; finally, our results are presented and summarized.

Electron Fokker-Planck and Cold-Ion Fluid Equations

Our model consists of a quasi-neutral homogeneous background plasma with fully ionized ions. The full electron FP operator is used, with the exception of *e-i* energy-exchange terms (which provide contributions of the order of $m_e/m_i << 1$). Adopting a perturbation of the electron distribution function of the form

$$f(x,\mathbf{v},t) = F_0(v) + \sum_{l=0}^{L} f_l(v,t)\,P_l(\mu)\exp(ikx), \qquad (1)$$

where $\mu = v_x/v$ and $P_l(\mu)$ is the lth Legendre mode, the linearized electron FP equation (defined in the rest frame of the ions) becomes[10]

$$\frac{\partial f_0}{\partial t} + \frac{ikv}{3} f_1 - \frac{iku_i}{3} v\frac{\partial F_0}{\partial v} = C_{ee}^i(F_0, f_0) + C_{ee}^i(f_0, F_0), \quad (2)$$

$$\frac{\partial f_1}{\partial t} + ikvf_0 + ikv\frac{2}{5}f_2 - \left(\frac{|e|E}{m_e} + \frac{\partial u_i}{\partial t}\right)\frac{\partial F_0}{\partial v}$$

$$= -\nu_{ei}f_1 + C_{ee}^i(F_0, f_1) + C_{ee}^a(F_0, f_1), \qquad (3)$$

$$\frac{\partial f_2}{\partial t} + \frac{2}{3}ikvf_1 + \frac{3}{7}ikvf_3 - \frac{2}{3}iku_i v\frac{\partial F_0}{\partial v}$$

$$= -3\nu_{ei}f_2 + C_{ee}^i(F_0, f_2) + C_{ee}^a(F_0, f_2), \qquad (4)$$

and

$$\frac{\partial f_l}{\partial t} + \frac{l}{2l-1}ikvf_{l-1} + \frac{l+1}{2l+3}ikvf_{l+1}$$

$$= -\frac{l(l+1)}{2}\nu_{ei}f_l + C_{ee}^i(F_0, f_l) + C_{ee}^a(F_0, f_l) \qquad (5)$$

for $l > 2$. The ion velocity u_i and electric field E are first order in the perturbation, and

$$F_0(v) = N_e\left(2\pi v_t^2\right)^{-3/2}\exp\left(-v^2/2v_t^2\right)$$

is an equilibrium Maxwellian, where N_e is the background electron number density, $v_t = \left(T_e/m_e\right)^{1/2}$ is the electron thermal velocity, and T_e is the electron temperature (in energy units). The velocity-dependent *e-i* collision frequency is given by

$$\nu_{ei}(v) = 4\pi N_e Z\left(e^2/m_e\right)^2 \ln\Lambda/v^3,$$

where e is the electron charge and $\ln\Lambda$ is the Coulomb logarithm (assumed the same for both electrons and ions). The terms C_{ee}^i and C_{ee}^a (defined in the Appendix) represent the isotropic and anisotropic parts of the *e-e* collision operator, respectively. Since the latter involves integration over the perturbed distribution function, it is usually neglected in FP calculations.[11] The validity of such approximation is the subject of "Approximations to the Fokker-Planck Equation" on p. 72.

The linearized cold-ion continuity and momentum equations are

$$\frac{\partial n_i}{\partial t} + ikN_i u_i = 0, \qquad (6)$$

and

$$N_i m_i\frac{\partial u_i}{\partial t} = ZN_i|e|E + R_{ie}, \qquad (7)$$

where $R_{ie} = (4\pi m_e/3)\int dv v^3 \nu_{ei} f_1$ is the *i-e* momentum exchange rate, n_i is the perturbed ion number density, and N_i is its background value. The perturbed electric field is calculated via Poisson's equation,

$$ikE = 4\pi|e|\left(Zn_i - n_e\right), \qquad (8)$$

where the perturbed electron number density is $n_e = 4\pi\int_0^\infty v^2 f_0 dv$.

Numerical Scheme (*SPRING* code)

A computer code (*SPRING*) has been written to solve Eqs. (2)–(8). It uses a "time-splitting" scheme with the following stages:

$$\frac{\partial f_1}{\partial t} = \left(\frac{|e|E}{m_e} + \frac{\partial u_i}{\partial t}\right)\frac{\partial F_0}{\partial v} \qquad \text{(acceleration)},$$

$$\frac{\partial f_0}{\partial t} = \frac{iku_i}{3} v \frac{\partial F_0}{\partial v} \qquad \text{(compression)},$$

$$\frac{\partial f_2}{\partial t} = \frac{2}{3} iku_i v \frac{\partial F_0}{\partial v} \qquad \text{(viscosity)},$$

$$\frac{\partial f_0}{\partial t} = C_{ee}^i(F_0, f_0) + C_{ee}^i(f_0, F_0)$$

$$\frac{\partial f_l}{\partial t} = C_{ee}^i(F_0, f_l) + C_{ee}^a(F_0, f_l) \qquad (e\text{-}e \text{ collision}),$$

and

$$\frac{\partial f_l}{\partial t} = -\frac{l}{2l-1} ikvf_{l-1} - \frac{l+1}{2l+3} ikvf_{l+1} - \frac{l(l+1)}{2} \nu_{ei} f_l$$

(advection and e-i angular scattering),

where $l > 0$. The acceleration, compression, and viscosity stages are advanced explicitly in time. In the e-e collision stage, the isotropic collision operators (which are differential operators) are evaluated implicitly using the Chang-Cooper[12] scheme, whereas the anisotropic operators (which are integral operators) are evaluated explicitly. In the advection-scattering stage, f_l is solved implicitly at each velocity group, using the boundary condition that $f_{-1} = f_{L+1} = 0$. The distribution function is defined on a velocity mesh with constant spacing of typically $\Delta v = 0.125 v_t$ between $v = 0$ and $6v_t$.

After advancing the distribution function in time, with a fixed time step Δt, the ion-fluid equations are solved explicitly. However, solving Poisson's equation explicitly to calculate E can lead to numerical instabilities when $\Delta t\, \omega_p > 1$ [where $\omega_p = \left(4\pi N_e e^2/m_e\right)^{1/2}$ is the plasma frequency]. To avoid this problem we use an implicit-moment method,[13] which involves taking density and momentum moments of the FP equation and substituting back into the ion continuity and Poisson's equations. An approximation to the electric field at a time $(t + \Delta t)$ can then be obtained from

$$ikE(t+\Delta t) = \frac{4\pi|e|}{\left(1+\omega_p^2 \Delta t^2\right)}\left\{Zn_i(t) - n_e(t) + ik\Delta t N_e \left[v_e(t) + ik\Delta t p(t)/N_e m_e - \Delta t R_{ie}(t)/N_e m_e\right]\right\}, \quad (9)$$

where $p = \left(4\pi m_e/3\right)\int dv v^4 f_0$ and $v_e = \left(4\pi/3N_e\right)\int dv v^3 f_1$. Since we are interested in low-frequency phenomena, such as sound waves, Eq. (9) allows us to use time steps larger than ω_p^{-1}.

The sound-wave eigenfrequencies are determined by appropriately initializing the dependent variables and monitoring their temporal evolution over several wave periods. In the past, simulations of this kind (involving the ion FP equation) have suffered from the occurrence of spurious transients that required complicated procedures to filter out the correct eigenfrequencies.[3] This problem appears to be associated with the fact that the "exact" perturbed eigenfunctions f_l are not known *a priori*. Rather than trying to guess f_l, a more satisfactory approach is to start with $f_l = n_i = 0$ and $u_i = 1$. The variables then typically converge to the appropriate eigenmodes within a few sound-wave periods. (An alternative approach based on eigenvalue analysis has also been proposed by Tracy *et al.*[4])

***SPRING* Simulation Results**

The code *SPRING* provides ion-acoustic damping rates γ/kc_s for different values of $k\lambda_{ei}$, $k\lambda_D$, Z, and A, where

$$\lambda_{ei} = 3T_e^2 \Big/ \left[4(2\pi)^{1/2} N_e Z e^4 \ln \Lambda\right],$$

$\lambda_D = v_t/\omega_p$ is the Debye length, A is the atomic mass, and $c_s = \left(ZT_e/m_i\right)^{1/2}$ is the isothermal sound speed. The code also calculates an effective thermal conductivity defined by $\kappa \equiv -q_{\mathrm{FP}}/ikT_{\mathrm{FP}}$, where

$$q_{\mathrm{FP}} = \left(2\pi m_e/3\right)\int dv\, v^5 f_1$$

is the electron heat flow and

$$T_{FP} = (4\pi m_e/N_e)\int dv\left(v^4/3 - v^2 v_t^{\,2}\right) f_0$$

is the temperature. Since we are primarily concerned with collisional effects, we choose $\lambda_D << k^{-1}$; also, for simplicity, we take $A = 2Z$.

1. Damping rate γ

The first test of *SPRING* involves neglecting *e-e* collisions altogether. This is equivalent to using the Lorentz plasma approximation, or high-Z limit, since $\nu_{ei}/\nu_{ee} \sim Z$. In this instance Eqs. (2)–(8) can be solved analytically by the method of continued fractions (see Ref. 1), and the results are plotted as curve *d* in Fig. 58.11. The code is found to reproduce these damping rates very accurately throughout the whole range of $k\lambda_{ei}$. (In practice, this requires using $Z >> 10^4$.)

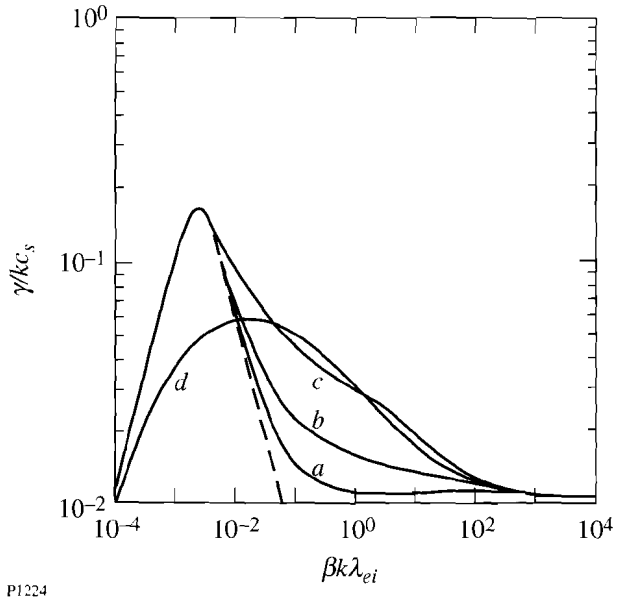

Figure 58.11
Plots of the damping rate of ion-acoustic waves γ/kc_s as functions of $\beta k\lambda_{ei}$, where c_s is the isothermal sound speed, k is the perturbation wave number, λ_{ei} is the electron-ion mean free path, and β is a scaling factor ($\beta = 0.24$, 0.68, 0.92, and 1 for $Z = 1$, 8, 64, and ∞, respectively). Solid curves represent *SPRING* simulations with (a) $Z = 1$, (b) $Z = 8$, (c) $Z = 64$, and (d) $Z = \infty$. The dashed curve refers to the fluid result.

To test the accuracy of the numerical implementation of the *e-e* operators we first consider the collisional case ($k\lambda_{ei} << 1$) with $Z = 1$. In this limit the Legendre expansion [Eq. (1)] can be truncated at $l = 1$, and f_0 approaches a perturbed Maxwellian. Since this is also the fluid limit, a sound-wave dispersion relation can be derived using the standard fluid equations (neglecting viscosity effects) with the Spitzer-Härm thermal conductivity $\kappa_{SH} = \gamma_0(Z) N_e v_t \lambda_{ei}$, where the Z-dependent, thermal-conductivity coefficient is approximately given by $\gamma_0(Z) \approx 3.20(0.24 + Z)/(1 + 0.24Z)$ and $\gamma_0(\infty) = 128/3\pi$. The resultant dispersion relation (using $\partial/\partial t = -i\omega$) is found to be

$$\left(\frac{\omega}{kc_s}\right)^2 = \frac{2}{3 + i\left(\frac{\omega}{kc_s}\right)3r} + 1 , \qquad (10)$$

where r is the ratio of the thermal diffusion rate $\left(2k^2\kappa_{SH}/3N_e\right)$ to the sound transit rate (kc_s) across k^{-1}. Since $r = 2\gamma_0 k\lambda_{ei}\left(m_i/Zm_e\right)^{1/2}/3$, it has been found convenient to plot γ/kc_s as a function of $\beta k\lambda_{ei}$, where

$$\beta = (A/2Z)^{1/2}\,\gamma_0(Z)/\gamma_0(\infty)$$

is a scaling factor of order unity. The damping rates based on Eq. (10) are plotted in Fig. 58.11 (dashed curve). *SPRING* simulation results are found to be in good agreement with these as $k\lambda_{ei} \to 0$.

Let us now consider the more interesting case of finite Z and $k\lambda_{ei}$. The results are shown in Fig. 58.11 (solid curves *a–c*) for $Z = 1$, 8, and 64. Starting from the large $k\lambda_{ei}$ limit, we note that the dominant collisional contribution comes from *e-i* collisions. [Here, a large number of Legendre modes are necessary to accurately model the damping (e.g., typically $L = 20$ for $\beta k\lambda_{ei} = 10^2$).] In the intermediate regime of $\beta k\lambda_{ei} \sim 1$ we find the peculiar result that *e-e* collisions actually reduce the damping rate. The reason for this becomes apparent if we consider the nature of the electron collisional process. As shown by Epperlein *et al.*[1] elastic scattering between electrons and ions gives rise to both sound-wave damping, through thermal diffusion, and sound-wave "undamping," through disruption of the Landau wave-particle interaction. However, the main collisional contribution between electrons is energy exchange, which acts to drive f_0 toward a perturbed Maxwellian. Hence, introducing *e-e* collisions can actually reduce the damping rate by bringing it closer to the fluid limit. Since $\nu_{ei}/\nu_{ee} \sim Z$, this effect is strongest for low-Z plasmas. (Although γ does not fall below γ_L for $\beta k\lambda_{ei} > 0.01$, if we artificially reduce the value of Z, we can effectively extend the "fluid limit" to larger values of $k\lambda_{ei}$ and thereby allow γ to be less than γ_L.)

To a lesser extent, *e-e* collisions also affect the anisotropic parts of the electron distribution function (i.e., $f_1, f_2, \ldots$). For example, the *e-e* collision terms on the RHS of Eq. (3) are responsible for reducing the thermal conductivity, thus giving rise to the Z-dependent thermal coefficient γ_0 in the fluid limit.

2. Approximations to the Fokker-Planck equation

The *e-e* collision operator for $l > 0$ (see Appendix) can be separated into an isotropic part $C_{ee}^{i}(F_0 f_l)$, which involves derivative operations on f_l, and an anisotropic part $C_{ee}^{a}(F_0 f_l)$, which involves integral operations on f_l. Since the latter is more difficult to implement numerically, it is usually neglected in electron FP calculations. Here we investigate the implications of neglecting both $C_{ee}^{a}(F_0 f_l)$ and $C_{ee}^{i}(F_0 f_l)$ for $l > 0$ and how we can simulate their effects by appropriately adjusting the value of ν_{ei}. We also briefly explore the possibility of using a generalized collision frequency to simulate the contribution from an infinite Legendre-mode expansion.

The effect of neglecting *e-e* collisions altogether (the so-called Lorentz approximation) has already been demonstrated in Fig. 58.11. There we see that apart from the weakly collisional regime $\beta k\lambda_{ei} >> 1$, where electron collisions play a relatively minor role in the sound-wave damping, or the strongly collisional regime $\left(\beta k\lambda_{ei} << 10^{-4}\right)$, where the thermal diffusion rate is much less than sound transit rate, it is not reasonable to neglect *e-e* collisions for $Z < 64$. This is especially true near the maximum value of γ/kc_s, at $\beta k\lambda_{ei} \approx 0.002$, where even for $Z = 64$ the Lorentz approximation leads to large errors.

The first approximation we consider uses isotropic Rosenbluth potentials only (i.e., setting $C_{ee}^{a} = 0$). Figure 58.12 shows a comparison of the damping rate (open circles) with the more accurate calculation discussed in the previous section. We note that the largest errors occur over the range $10^{-1} < \beta k\lambda_{ei} < 10^{1}$ with an overall maximum of about 10%. Since the relative contribution from *e-e* collisions is most significant for low Z, the worst possible case occurs with $Z = 1$.

The second approximation neglects *e-e* collisions altogether for $l > 0$ (i.e., setting $C_{ee}^{i} = C_{ee}^{a} = 0$ for $l > 0$). To offset this more drastic approximation we introduce a modified collision frequency $\nu_{ei}^{*} = \left[\gamma_0(\infty)/\gamma_0(Z)\right]\nu_{ei}$. The new factor $\left[\gamma_0(\infty)/\gamma_0(Z)\right] \approx (Z + 4.2)/(Z + 0.24)$ has the effect of giving the correct (SH) thermal conductivity in the collisional limit. A plot of the corresponding damping rate for $Z = 1$ (the crosses in Fig. 58.12) shows that, once again, the errors are larger at intermediate values of $\beta k\lambda_{ei}$ with a maximum of about 10%. As in the previous case, this low-Z example provides the worst possible case.

The advantage of neglecting *e-e* collisions for $l > 0$ (through the introduction of ν_{ei}^{*}) is that Eqs. (3)–(5) become algebraic in v, allowing for much faster numerical solution of the coupled equations.

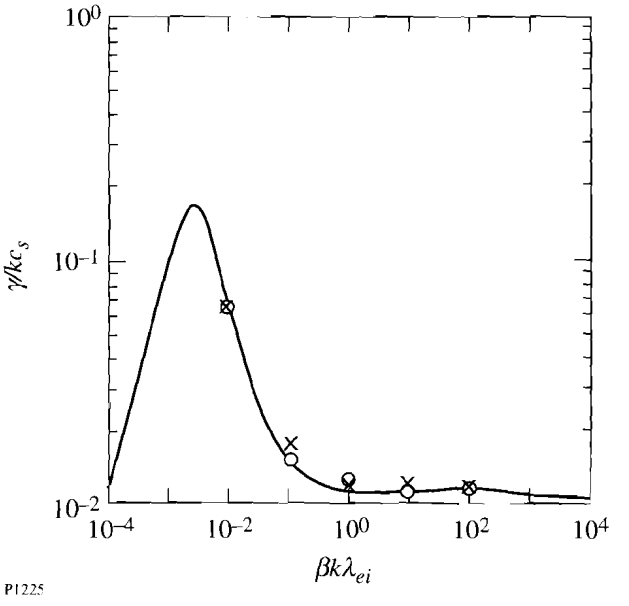

Figure 58.12
Plots of the damping rate of ion-acoustic waves γ/kc_s as functions of $\beta k\lambda_{ei}$ for $Z = 1$ (as in Fig. 58.11). Results using isotropic Rosenbluth potentials are displayed as open circles, whereas those using ν_{ei}^{*} are displayed as crosses.

Provided we are only interested in low-frequency waves [such that $\omega << \nu_{ei}(v_t)$], we can now go a step further and use the techniques of Ref. 1 to reduce Eqs. (3)–(5) to a single equation,

$$ikvf_0 - \left[\frac{|e|E}{m_e} + \frac{\partial u_i}{\partial t} + \left(\nu^* - \nu_{ei}^*\right)u_i\right]\frac{\partial F_0}{\partial v} = -\nu^* f_1 . \quad (11)$$

Here, $\nu^*(k) = \nu_{ei}^*\left[1 + \left(\pi kv/6\nu_{ei}^*\right)^2\right]^{1/2}$ is the low-frequency-generalized collision frequency proposed by Epperlein *et al.*,[1] which incorporates the contribution from all Legendre modes with $l > 1$. By substituting Eq. (11) into Eq. (2), we are left with a single differential equation for f_0, which is easier to solve than the original set of coupled equations. However, a discussion of the numerical methods involved is outside the scope of this article.

3. Effective thermal conductivity κ

Figure 58.13 plots (a) $|\kappa/\kappa_{SH}|$ and (b) $\arg(\kappa)$ as functions of $\beta k\lambda_{ei}$ for $Z = 1$, 8, 64, and ∞ (solid curves). The dashed curve shows the results of Hammett and Perkins (for a collisionless plasma).

When neglecting e-e collisions (Lorentz plasma approximation), our results agree with the analytic solutions of Ref. 1. In the collisional limit $(k\lambda_{ei} << 1)$, we have $\kappa = \kappa_{SH}$, whereas in the collisionless limit $(k\lambda_{ei} >> 1)$, we have $\kappa = \kappa_{HP} = 3(2/\pi)^{1/2} N_e v_t/|k|$ [see dashed curve HP in Fig. 58.13(a)]. (The formula for κ_{HP} is 1.5 times larger than the one used by Hammett and Perkins since ours is defined in terms of the isotropic temperature T_{FP}.) Comparing our results with those of Chang and Callen,[8] however, we find considerable discrepancy in the $k\lambda_{ei} << 1$ limit. Although the authors point out in their paper that they underestimate the thermal conductivity by a factor of 2.4 for $Z = 1$, this factor actually rises up to 7.1 for $Z >> 1$.

Two mechanisms can be identified that reduce the heat flow below the SH limit, q_{SH}. The first one is caused by a departure of f_0 from the perturbed Maxwellian.[14] When the mean free path of heat-carrying electrons (with velocities close to 3.6 v_t) becomes greater than k^{-1}, their spatial gradient in configuration space is reduced. Since these relatively collisionless electrons cannot thermalize instantaneously with thermal electron population (as required by fluid theory), the heat flow is reduced below q_{SH}. The reduction in heat flow is therefore governed by the balance between the thermal-diffusion rate and the e-e thermalization rate [as given by the collision term in Eq. (2)]. In the Lorentz plasma approximation, where e-e collisions are neglected altogether, there is no effective coupling between different electron-energy groups, as illustrated by the large phase shift between q_{FP} and T_{FP} in Fig. 58.13(b). As seen in Figs. 58.13(a) and 58.13(b), the departure from fluid theory then becomes significant when $r \sim k\lambda_{ei}(m_i/Zm_e)^{1/2} > 1$, i.e., when the thermal-diffusion time becomes less than the hydrodynamic time. As e-e collisions are introduced (identified by the finite-Z curves), f_0 is driven closer to a perturbed Maxwellian and the onset of kinetic effects is shifted to larger values of $k\lambda_{ei}$. The phase difference between q_{FP} and T_{FP} is also considerably reduced by the introduction of e-e collisions and becomes negligible for $Z = 1$ [see Fig. 58.13(b)].

Regardless of the e-e thermalization strength, the electron heat flow cannot exceed the "free-streaming," or collision-

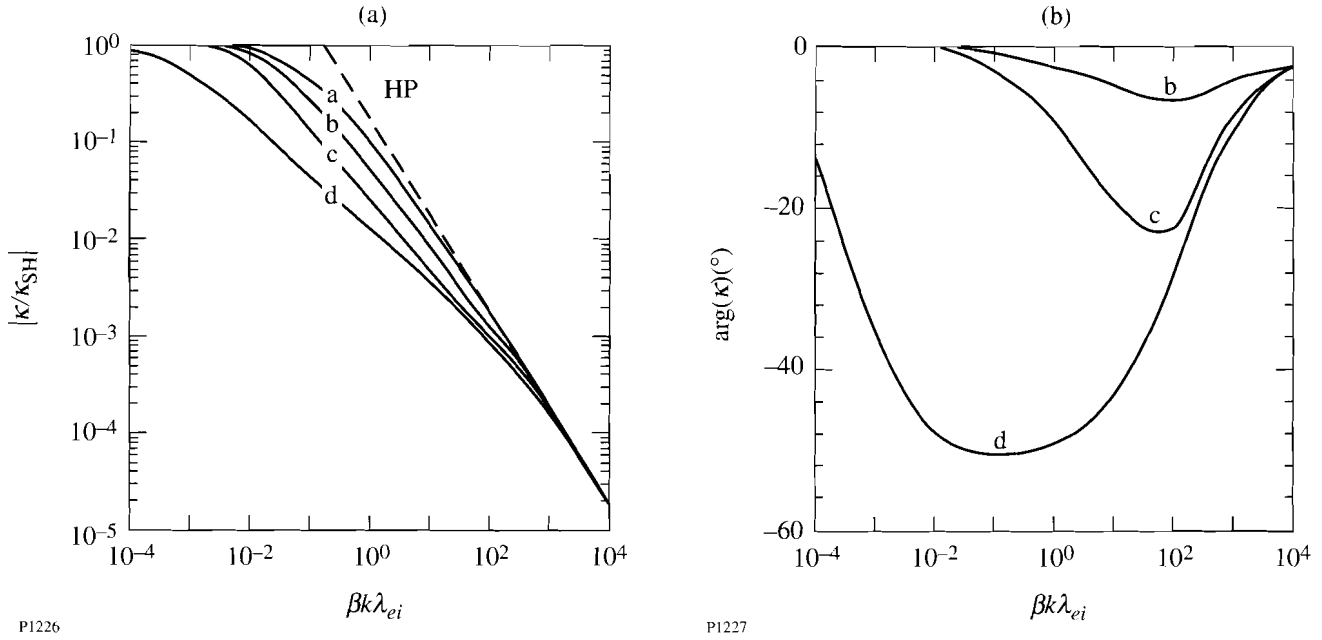

Figure 58.13
Plots of (a) $|\kappa/\kappa_{SH}|$ and (b) $\arg(\kappa)$ as functions of $\beta k\lambda_{ei}$, where κ and κ_{SH} are the effective and Spitzer-Härm thermal conductivities, respectively. As in Fig. 58.11, the solid curves refer to *SPRING* simulation results with (a) $Z = 1$, (b) $Z = 8$, (c) $Z = 64$, and (d) $Z = \infty$ [for $Z = 1$, $\arg(\kappa) << 1$]. Here the dashed curve refers to the model of Hammett and Perkins.

less, limit as calculated by Hammett and Perkins,[7] i.e., $q_{HP} = -(ik/|k|)3(2/\pi)^{1/2} N_e T_{FP} v_t$. This gives us the second mechanism for the reduction of κ, with the upper limit shown by the plot of $\kappa_{HP}/\kappa_{SH} = 9(2\pi)^{1/2}(A/2Z)^{1/2}/(128\beta k\lambda_{ei})$ (dashed curve) in Fig. 58.13(a).

Other processes can also affect the electron thermal conductivity. Inverse-bremsstrahlung heating, for example, preferentially heats low-velocity electrons, which in turn modifies f_0 and leads to even further reduction of κ.[9] Such a phenomenon has been recently investigated and shown to have a significant impact on both filamentation[9] and stimulated Brillouin scattering[15] in laser-produced plasmas. The corresponding values of κ have been calculated using the nonlinear FP code *SPARK*; the following analytical fit to the simulation results has been proposed:[9]

$$\frac{\kappa_{IB}}{\kappa_{SH}} = \frac{1}{1+(30k\lambda_e)^{4/3}}, \qquad (12)$$

where $\lambda_e = \eta T^2/\left[4\pi N_e e^4 Z^{1/2} \ln\Lambda\right]$ is the electron delocalization length and $\eta = \left[\gamma_0(Z)/\gamma_0(\infty)\right]^{1/2}$. (As observed in Ref. 9, certain care is needed in defining Z for multispecies ions.) The resulting dashed curve (IB) for $Z = 1$ is plotted in Fig. 58.14 as a function of $\beta k\lambda_{ei}$. Although the original simulation results were based on a two-Legendre-mode expansion for the distribution function (i.e., $L = 1$), the contribution from higher-order modes have been investigated by Epperlein and Short[6] [using a generalized collision frequency ν^* of the type discussed in "Approximations to the Fokker-Planck equation"] and found to be negligible.

Here, we are able to check on the accuracy of Eq. (12) by using *SPRING* with an inverse-bremsstrahlung heating source of the type[16]

$$\frac{1}{v^2}\frac{\partial}{\partial v}\left(\frac{g}{v}\frac{\partial f_0}{\partial v}\right)$$

inserted on the right-hand side of Eq. (2), where

$$g = \left[1+(\nu_{ei}/\omega_0)^2\right]^{-1}$$

and ω_0 is the light-wave frequency. The code is then run until the distribution function reaches a steady state. In this case, ion motion does not play a significant role. The corresponding values of κ/κ_{SH} (also for $Z = 1$) have been calculated for range of $bk\lambda_{ei}$ and displayed as circles in Fig. 58.14. As shown, the simple analytic fit [Eq. (12)] can accurately reproduce the more accurate *SPRING* simulation results. For comparison, the values of κ for an undriven plasma [curve Z = 1 in Fig. 58.13(a)] has also been plotted in Fig. 58.14.

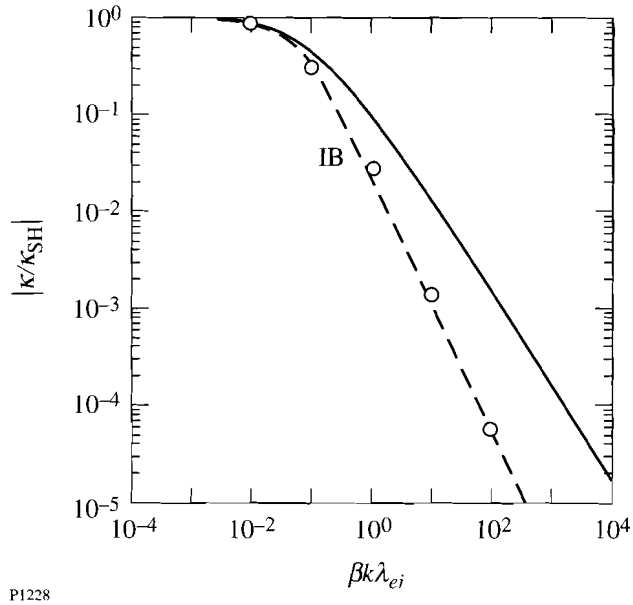

Figure 58.14
Plot of κ/κ_{SH} as a function of $\beta k\lambda_{ei}$ for $Z = 1$ (as in Fig. 58.13). Here the dashed curve refers to the analytic formula for κ_{IB} (from Ref. 9), and circles represent *SPRING* simulation results with an inverse-bremsstrahlung heating source.

Summary

The effect of electron collisionality on the damping of ion-acoustic waves has been investigated by numerically solving the electron FP and cold-ion-fluid equations. The code (*SPRING*) developed for this purpose reproduces the analytic results previously obtained for a Lorentz plasma (i.e., without *e-e* collisions).

The introduction of *e-e* collisions shows that the Lorentz approximation is inadequate near the peak of the damping rate at $k\lambda_{ei} \sim (Zm_e/m_i)^{1/2}$. For $k\lambda_{ei} > (Zm_e/m_i)^{1/2}$ and $Z < 64$, *e-e* collisions reduce the damping rate below the Lorentz value, though it still remains higher than the γ_{fluid} and γ_L.

A convenient approximation that involves adjusting the *e-i* collision frequency to model the contribution from *e-e* collisions for $l > 1$ has been found to yield errors of up to 10% in the damping rate. A further generalization of the *e-i* collision

frequency that simulates the contribution from all Legendre modes with $l > 1$ has also been discussed.

Calculations of the effective thermal conductivity κ for a Lorentz plasma have shown significant reduction from the Spitzer-Härm value κ_{SH} for $k\lambda_{ei} > 10^{-4}$. However, even for Z as high as 64, e-e collisions extend the validity of the fluid approximation for up to $k\lambda_{ei} \sim 10^{-2}$. In the limit as $k\lambda_{ei} \to \infty$, κ approaches the value $3(2/\pi)^{1/2} N_e v_t / k$ predicted by Hammett and Perkins.

Heating the plasma with a spatially modulated inverse-bremsstrahlung heating source, and solving for the steady-state distribution function, has been shown to further reduce κ. The accuracy of a simple analytic formula previously derived for κ_{IB} has been verified for up to $k\lambda_{ei} \sim 10^{-2}$.

ACKNOWLEDGMENT

The author acknowledges many useful discussions with Robert W. Short, Albert Simon, and Mark D. Tracy. This work was supported by the U.S. Department of Energy Office of Inertial Confinement Fusion under Cooperative Agreement No. DE-FC03-92SF19460, the University of Rochester, and the New York State Energy Research and Development Authority. The support of DOE does not constitute an endorsement by DOE of the views expressed in this article.

APPENDIX: THE ELECTRON-ELECTRON COLLISION OPERATOR

The isotropic and anisotropic parts of the collision operator are given by[2,10]

$$C_{ee}^{i}(f_0, f_l) = \nu_{ee} v \frac{\partial}{\partial v}\left[f_l I_0^0 + \frac{v}{3}\frac{\partial f_l}{\partial v}\left(I_2^0 + J_{-1}^0\right)\right]$$

and

$$C_{ee}^{a}(f_0, f_l)$$

$$= \nu_{ee}\left\{ 4\pi v^3 f_l f_0 + \frac{l(l+1)}{6} f_l\left(-3I_0^0 + I_2^0 - 2J_{-1}^0\right)\right.$$

$$+\frac{v^2}{2(2l+1)}\frac{\partial^2 f_0}{\partial v^2}\left[\frac{(l+2)(l+1)}{2l+3}\left(I_{l+2}^{l} + J_{-1-l}^{l}\right)\right.$$

$$\left.-\frac{l(l-1)}{2l-1}\left(I_l^l + J_{1-l}^l\right)\right]$$

$$+\frac{v}{2(2l+1)}\frac{\partial f_0}{\partial v}\left[-\frac{(l+1)(l+2)}{(2l+3)} I_{l+2}^{l} - \frac{\left(l^2-l-4\right)}{(2l+3)} J_{-1-l}^{l}\right.$$

$$\left.\left.+\frac{\left(l^2+3l-2\right)}{(2l-1)} + \frac{l(l-1)}{(2l-1)} J_{1-l}^{l}\right]\right\},$$

where

$$I_m^n = \frac{4\pi}{v^m}\int_0^v f_n w^{2+m} dw,\ J_m^n = \frac{4\pi}{v^m}\int_v^\infty f_n w^{2+m} dw$$

and $\nu_{ee}(v) = 4\pi N_e\left(e^2/m_e\right)^2 \ln\Lambda / v^3$ is the velocity-dependent e-e collision frequency. Here we note that $C_{ee}^{i}(f_0, f_0) = C_{ee}^{a}(f_0, f_0)$.

REFERENCES

1. E. M. Epperlein, R. W. Short, and A. Simon, Phys. Rev. Lett. **69**, 1765 (1992).
2. M. N. Rosenbluth, W. M. MacDonald, and D. L. Judd, Phys. Rev. **107**, 1 (1957).
3. C. J. Randall, Phys. Fluids **25**, 2231 (1982).
4. M. D. Tracy, E. A. Williams, K. G. Estabrook, J. S. DeGroot, and S. M. Cameron, Phys. Fluids B **5**, 1430 (1993).
5. L. Spitzer, Jr. and R. Härm, Phys. Rev. **89**, 977 (1953).
6. E. M. Epperlein and R. W. Short, Phys. Fluids B **3**, 3092 (1991).
7. G. W. Hammett and F. W. Perkins, Phys. Rev. Lett. **64**, 3019 (1990).
8. Z. Chang and J. D. Callen, Phys. Fluids B **4**, 1167 (1992); Phys. Fluids B **4**, 1182 (1992)
9. E. M. Epperlein, Phys. Rev. Lett. **65**, 2145 (1990); E. M. Epperlein and R. W. Short, Phys. Fluids B **4**, 2211 (1992).
10. I. P. Shkarofsky, T. W. Johnston, and M. A. Bachynski, *The Particle Kinetics of Plasmas* (Addison-Wesley, Reading, MA, 1966); T. W. Johnston, J. Math. Phys. **7**, 1453 (1966).
11. E. M. Epperlein, *Laser and Particle Beams* **12**, 257 (1994).
12. J. S. Chang and G. Cooper, J. Comput. Phys. **6**, 1 (1970).
13. R. J. Mason, J. Comput. Phys. **41**, 233 (1981).
14. A. R. Bell, Phys. Fluids **26**, 279 (1983).
15. R. W. Short and E. M. Epperlein, Phys. Rev. Lett. **68**, 3307 (1992); H. A. Rose and D. F. DuBois, Phys. Fluids B **4**, 1394 (1992); E. M. Epperlein and R. W. Short, Phys. Fluids B **4**, 4190 (1992); H. A. Rose and D. F. DuBois, Phys. Fluids B **4**, 4192 (1992).
16. A. B. Langdon, Phys. Rev. Lett. **44**, 575 (1980).